Contribution from the Department of Inorganic Chemistry, Indian Association for the Cultivation of Science, Calcutta 700 032, India

Nickel(III)-Sulfur Binding. Chemistry of the Tris(xanthate) Family

Suranjan Bhanja Choudhury, Debashis Ray, and Animesh Chakravorty*

Received April 2, 1990

Tris(xanthates) of trivalent nickel, $Ni(Rx)_3$ (**2**, R = Me, Et, *n*-Pr, *i*-Pr, *n*-Bu, *i*-Bu, *s*-Bu), are quantitatively generated in acetonitrile solution by electrooxidation of $Ni(Rx)_3^-$ (**1**). The nickel(III)-nickel(II) formal potentials are in the range 0.1-0.16 V vs SCE (298 K). The X-ray structure of one nickel(II) precursor complex, $[Et_4N][Ni(Etx)_3]$, is reported: space group $P2_1/n$, $Z = 8$, $a = 18.842$ (7) Å, $b = 16.448$ (4) Å, $c = 18.987$ (7) Å, $\beta = 115.65$ (3)°, $V = 5304$ (3) Å^3, $R = 0.0484$, $R_w = 0.0578$. The anionic NiS_6 coordination sphere has approximate 3-fold symmetry with an average Ni-S distance of 2.439 (2) Å. Solutions of $Ni(Rx)_3$ undergo facile disproportionation: $2Ni(Rx)_3 \rightleftharpoons 2Ni(Rx)_2 + R_2x_2$. For R = Et the equilibrium constant is 391 L mol^{-1} at 298 K. The forward reaction is first order ($k = 1.0 \times 10^{-3}$ s^{-1} at 253 K; $\Delta S^{\ddagger} \sim -40$ eu) and is believed to proceed via the transition state $Ni(Etx)_2(Etx^{\bullet})$. Significant concentrations of $Ni(Etx)_3$ can be generated in solution via oxidative addition of Et_2x_2 (excess) to $Ni(Etx)_2$. By crystallization of $Co(Rx)_3$ from such solutions, 1 mole % of $Ni(Rx)_3$ has been substitutionally incorporated into the cobalt(III) lattice. The nickel(III) EPR spectrum of the polycrystalline doped lattice at 77 K is axial due to the dictates of crystal symmetry: $g_{\perp} = 2.099$, $g_{\parallel} = 2.082$. The expected Jahn-Teller distortion (low spin d^7) becomes observable in glassy solutions (77 K): $g_1 = 2.141$, $g_2 = 2.124$, $g_3 = 2.035$. A free energy cycle (298 K) has been constructed, incorporating the disproportionation reaction along with the following processes: $Ni(Etx)_2 + Etx^- \rightleftharpoons Ni(Etx)_3^-$ ($K = 10^5$ L mol^{-1}); $Etx^{\bullet} + e \rightleftharpoons Etx^-$ ($E^{\circ} = 0.23$ V); $2Etx^{\bullet} \rightleftharpoons Et_2x_2$ ($K = 4.56 \times 10^{16}$ L mol^{-1}); $Ni(Etx)_3 + e \rightleftharpoons Ni(Etx)_3^-$ ($E^{\circ} = 0.11$ V). The corresponding cycle for cognate dithiocarbamate species is also given for comparison. The analysis reveals that, in fluid media containing sulfur in oxidation states -2 (as in Rx^-) and 0 (as in R_2x_2), the bivalent and trivalent states of nickel appear as natural thermodynamic entities. The factors that favor the $Ni^{III}S$- species are noted. Disproportionation is effectively hindered by lowering the nickel(III)-nickel(II) reduction potential. The significance of these results in relation to nickel-containing hydrogenases is noted. It is proposed that nickel-sulfur systems containing the metal in the formally trivalent state can be described as resonance hybrids of the canonical forms Ni^{III}-S- and Ni^{II}-S$^{\bullet}$-, the latter approximating the transition state of disproportionation.

Introduction

The chemistry of trivalent nickel coordinated to nitrogen and/or oxygen donor ligands has received considerable attention during the past two decades.[1,2] In contrast, progress in the nickel(III) chemistry of classical sulfur donor ligands has been tardy. Recently we showed[3,4] that certain triazene 1-oxide thioether complexes of coordination type $Ni^{II}N_2O_2S_2$ can be electrooxidized in solution to EPR-characterizable, albeit unstable, nickel(III) congeners. Prior to this, nickel(III)-sulfur binding was documented in few systems outside dithiocarbamates.[1a,5,6] Subsequent to our work,[3] examples of thiolate coordination to nickel(III) have appeared.[7,8] All nickel(III)-sulfur species examined so far are unstable, and isolation of a pure entity remains elusive. Current interest in oxidized sulfur-ligated nickel systems originates from their potential usefulness as synthetic models of the trivalent centers of nickel-containing hydrogenases.[9,10]

Table I. Electrochemical Data[a,b] at 298 K

R	KRx Rx^0/Rx^- $E^{\circ}(2)$,[c] V	$Ni(Rx)_3^-$ Ni^{III}/Ni^{II} $E^{\circ}(4)$,[d] V	$Ni(Rx)_3^-$ Ni^{III}/Ni^{II} n (E, V)[e,f]	Ni^{IV}/Ni^{III} $E_{pa}(5)$,[c] V
Me	0.24	0.16	0.98 (0.40)	0.73
Et	0.23	0.11	0.97 (0.35)	0.72
n-Pr	0.25	0.11	1.02 (0.35)	0.69
i-Pr	0.26	0.10	0.93 (0.35)	0.68
n-Bu	0.28	0.11	0.98 (0.40)	0.67
i-Bu	0.26	0.10	1.03 (0.35)	0.71
s-Bu	0.25	0.10	0.96 (0.35)	0.70

[a] Unless otherwise stated, the meanings of the symbols are the same as in the text. [b] The solvent is acetonitrile, the supporting electrolyte is TEAP (0.1 M), the working electrode is platinum, the reference electrode is the SCE, and the scan rate is 50 mV s^{-1}. [c] E° calculated by subtracting 30 mV from observed E_{pa}. [d] E° calculated as the average of anodic and cathodic peak potentials. [e] Constant-potential coulometric data. [f] $n = Q/Q'$, where Q is the observed coulomb count and Q' is the calculated coulomb count for one-electron transfer; E is the constant potential at which electrolysis was performed.

(1) (a) Nag, K.; Chakravorty, A. *Coord. Chem. Rev.* **1980**, *33*, 87-147. (b) Haines, R. I.; McAuley, A. *Coord. Chem. Rev.* **1981**, *39*, 77-119. (c) Chakravorty, A. *Isr. J. Chem.* **1985**, *25*, 99-105. (d) Chakravorty, A. *Comments Inorg. Chem.* **1985**, *4*, 1-16. (e) Bhattacharya, S.; Mukherjee, R. N.; Chakravorty, A. *Inorg. Chem.* **1986**, *25*, 3448-3452. (f) Ray, D.; Chakravorty, A. *Inorg. Chem.* **1988**, *27*, 3292-3297. Recent contributions to higher oxidation states of nickel were extensively cited in the last two references. Subsequent progress in nickel(III) coordination chemistry is referenced below.[2]

(2) Amine and peptide complexes: (a) Fox, D.; Wells, C. F. *J. Chem. Soc., Dalton Trans.* **1989**, 151-154. (b) Wang, J.-F.; Kumar, K.; Mergerum, D. W. *Inorg. Chem.* **1989**, *28*, 3481-3484. Macrocyclic and diketonato complexes: (c) Fabbrizzi, L.; Mariani, M.; Seghi, B.; Zanchi, F. *Inorg. Chem.* **1989**, *28*, 3362-3366. (d) Katsuyama, T.; Bakac, A.; Espenson, J. H. *Inorg. Chem.* **1989**, *28*, 339-341. (e) Santis, G. D.; Casa, M. D.; Mariani, M.; Seghi, B.; Fabbrizzi, L. *J. Am. Chem. Soc.* **1989**, *111*, 2422-2427. (f) Yamashita, M.; Miyamae, H. *Inorg. Chim. Acta* **1989**, *156*, 71-75. (g) Bradbury, J. R.; Hampton, J. L.; Martone, D. P.; Maverick, A. W. *Inorg. Chem.* **1989**, *28*, 2392-2399. Dithiolene complexes: (h) Clemensen, P. I.; Underhill, A. E.; Hursthouse, M. B.; Short, R. L. *J. Chem. Soc., Dalton Trans.* **1989**, 1689-1692.

(3) Ray, D.; Pal, S.; Chakravorty, A. *Inorg. Chem.* **1986**, *25*, 2674-2676.

(4) One of the species has now been characterized by X-ray structure determination: Bhanja Choudhury, S.; Ray, D.; Chakravorty, A. Unpublished results.

(5) (a) Hendrickson, A. R.; Martin, R. L.; Rohde, N. M. *Inorg. Chem.* **1975**, *14*, 2980-2985. (b) Lachenal, D. *Inorg. Nucl. Chem. Lett.* **1975**, *11*, 101-106. (c) Solozhenkin, P. M.; Kopitsya, N. I. *Dokl. Akad. Nauk Tadzh. SSR* **1969**, *12*, 30-32.

(6) The 1,2-dithiolene type species are excluded because of their highly delocalized nature.[1a] Recent reports: (a) Welch, J. H.; Bereman, R. D.; Singh, P. *Inorg. Chem.* **1988**, *27*, 3680-3682. (b) Schultz, A. J.; Wang, H. H.; Soderholm, L. C.; Sifter, T. L.; Williams, J. M.; Bechgaard, K.; Whangbo, M.-H. *Inorg. Chem.* **1987**, *26*, 3757-3761. (c) Vance, C. T.; Bereman, R. D.; Bordner, J.; Hatfield, W. E.; Helms, J. H. *Inorg. Chem.* **1985**, *24*, 2905-2910.

(7) Electrochemical and EPR evidence: (a) Krüger, H.-J.; Holm, R. H. *Inorg. Chem.* **1987**, *26*, 3645-3647. (b) Kumar, M.; Day, R. O.; Colpas, G. J.; Maroney, M. J. *J. Am. Chem. Soc.* **1989**, *111*, 5974-5976. (c) Fabbrizzi, L.; Prosperpio, D. M. *J. Chem. Soc., Dalton Trans.* **1989**, 229-232. (d) Fortier, D. G.; McAuley, A. *Inorg. Chem.* **1989**, *28*, 655-662.

(8) Electrochemical evidence only: (a) Baidya, N.; Olmstead, M. M.; Mascharak, P. K. *Inorg. Chem.* **1988**, *27*, 3426-3432. (b) Bond, A. M.; Haga, M.-A.; Creece, I. S.; Robson, R.; Wilson, J. C. *Inorg. Chem.* **1988**, *27*, 712-721.

(9) Lancaster, J. R., Jr. *The Bioinorganic Chemistry of Nickel*; VCH Publishers: New York, 1988.

(10) (a) Lancaster, J. R., Jr. *Science (Washington, D.C.)* **1982**, *216*, 1324-1325. (b) Thomson, A. J. *Nature (London)* **1982**, *298*, 602-603. (c) Fangue, G.; Peck, H. D., Jr.; Moura, J. J. G.; Huynh, B. H.; Berlier, Y.; DerVartanian, D. V.; Teixeira, M.; Przbyla, A. E.; Lespinat, P. A.; Moura, I.; LeGall, J. *FEMS Microbiol. Rev.* **1988**, *54*, 299-344. (d) Kowal, A. J.; Zambrano, I. C.; Moura, I.; Moura, J. J. G.; LeGall, J.; Johnson, M. K. *Inorg. Chem.* **1988**, *27*, 1162-1166 and references therein.

0020-1669/90/1329-4603$02.50/0

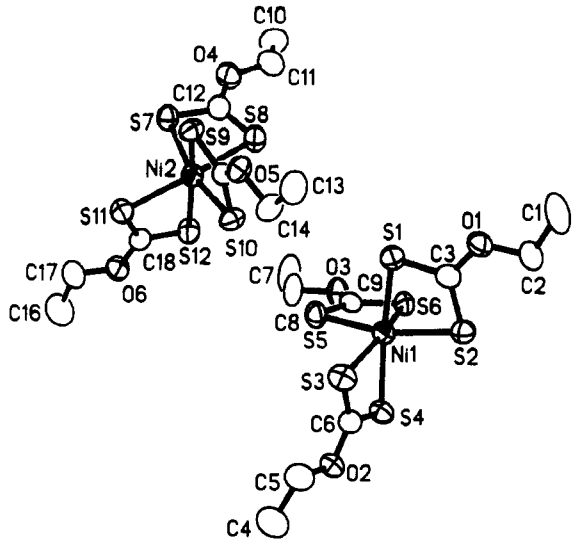

Figure 1. ORTEP plot and labeling scheme of the asymmetric unit (anions only) of $[Et_4N][Ni(Etx)_3]$. All atoms are represented by their 50% probability ellipsoids.

In this work we examine tris chelate binding of trivalent nickel by the xanthates, $ROC(S)S^-$ (abbreviated Rx^-). The corresponding bivalent species $Ni(Rx)_3^-$ are used as precursors for electrogeneration of $Ni^{III}(Rx)_3$. The X-ray structure of one nickel(II) complex (R = Et) has been determined, and the nature and reactions of $Ni(Rx)_3$ are probed by EPR and voltammetric techniques. In solution $Ni(Rx)_3$ undergoes spontaneous and reversible disproportionation to the nickel(II) bis complex, $Ni(Rx)_2$, and dixanthogen, $ROC(S)SS(S)COR$ (R_2x_2). The free energy terms driving this reaction are examined with the help of a thermodynamic cycle. Disproportionation has vitiated attempts for isolation of $Ni(Rx)_3$ in the pure state. It has however been possible to substitutionally incorporate the trivalent complex into the corresponding cobalt(III) lattice, and in this condition $Ni(Rx)_3$ is indefinitely stable.

Results

A. Nickel(II) Precursors. a. Synthesis and Equilibria. The green paramagnetic ($S = 1$) tris chelate anion[11] $Ni(Rx)_3^-$ (**1**, isolated its Et_4N^+ salt) and the brown diamagnetic bis complex[12]

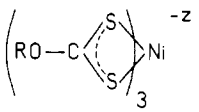

1 z = 1

2 z = 0

$Ni(Rx)_2$ are formed by stoichiometric reactions of nickel(II) salts with potassium xanthate in aqueous solution. The complexes of type **1** used in the present study are listed in Table I. Among these, the R = Me and Et species have been reported earlier.[11]

When potassium xanthate is added to $Ni(Rx)_2$ in acetonitrile, the tris chelate is formed (eq 1). The equilibrium constant, $K(1)$,

$$Ni(Rx)_2 + Rx^- \overset{K(1)}{\rightleftharpoons} Ni(Rx)_3^- \qquad (1)$$

is estimated for the case of R = Et by using the ligand field band[11a] intensity of $Ni(Etx)_3^-$. Tris chelate formation is a highly favorable process with $K(1) > 10^5$ L mol^{-1} at 298 K.

b. Structure of $[Et_4N][Ni(Etx)_3]$. The asymmetric unit consists of two closely similar but independent molecules, as shown in Figure 1 (complex anions only) along with the atom-numbering scheme. The disposition of anions and cations is displayed in the packing diagram of Figure 2. Selected bond distances and angles are listed in Table II.

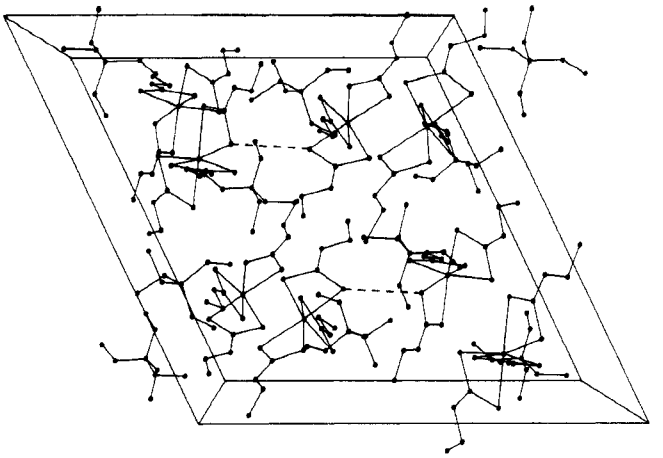

Figure 2. Cell packing diagram of $[Et_4N][Ni(Etx)_3]$, viewed down the *b* axis.

Table II. Selected Bond Distances (Å) and Angles (deg) and Their Estimated Standard Deviations for $[Et_4N][Ni(Etx)_3]$[a]

Distances			
Ni(1)–S(1)	2.434 (2)	Ni(2)–S(7)	2.437 (2)
Ni(1)–S(2)	2.446 (2)	Ni(2)–S(8)	2.448 (2)
Ni(1)–S(3)	2.455 (2)	Ni(2)–S(9)	2.427 (2)
Ni(1)–S(4)	2.428 (2)	Ni(2)–S(10)	2.428 (2)
Ni(1)–S(5)	2.419 (2)	Ni(2)–S(11)	2.448 (2)
Ni(1)–S(6)	2.452 (2)	Ni(2)–S(12)	2.438 (2)
S(1)–C(3)	1.681 (7)	S(7)–C(12)	1.690 (7)
S(2)–C(3)	1.680 (7)	S(8)–C(12)	1.673 (7)
S(3)–C(6)	1.675 (8)	S(9)–C(15)	1.684 (6)
S(4)–C(6)	1.687 (7)	S(10)–C(15)	1.676 (7)
S(5)–C(9)	1.689 (6)	S(11)–C(18)	1.689 (8)
S(6)–C(9)	1.672 (6)	S(12)–C(18)	1.680 (7)
O(1)–C(2)	1.470 (9)	O(4)–C(11)	1.449 (9)
O(1)–C(3)	1.338 (8)	O(4)–C(12)	1.332 (7)
O(2)–C(5)	1.459 (8)	O(5)–C(14)	1.469 (8)
O(2)–C(6)	1.339 (7)	O(5)–C(15)	1.336 (6)
O(3)–C(8)	1.459 (9)	O(6)–C(17)	1.441 (9)
O(3)–C(9)	1.337 (6)	O(6)–C(18)	1.330 (8)
Angles			
S(1)–Ni(1)–S(2)	73.3 (1)	S(3)–Ni(1)–S(5)	92.9 (1)
S(1)–Ni(1)–S(3)	97.8 (1)	S(4)–Ni(1)–S(5)	92.9 (1)
S(2)–Ni(1)–S(3)	100.6 (1)	S(1)–Ni(1)–S(6)	95.9 (1)
S(1)–Ni(1)–S(4)	166.8 (1)	S(2)–Ni(1)–S(6)	95.0 (1)
S(2)–Ni(1)–S(4)	98.5 (1)	S(3)–Ni(1)–S(6)	161.6 (1)
S(3)–Ni(1)–S(4)	73.2 (1)	S(4)–Ni(1)–S(6)	95.1 (1)
S(1)–Ni(1)–S(5)	97.3 (1)	S(5)–Ni(1)–S(6)	73.2 (1)
S(2)–Ni(1)–S(5)	164.4 (1)	S(7)–Ni(2)–S(8)	73.0 (1)
S(7)–Ni(2)–S(9)	95.3 (1)	S(9)–Ni(2)–S(11)	98.3 (1)
S(8)–Ni(2)–S(9)	93.0 (1)	S(10)–Ni(2)–S(11)	97.1 (1)
S(7)–Ni(2)–S(10)	163.9 (1)	S(7)–Ni(2)–S(12)	96.3 (1)
S(8)–Ni(2)–S(10)	95.5 (1)	S(8)–Ni(2)–S(12)	97.5 (1)
S(9)–Ni(2)–S(10)	73.6 (1)	S(9)–Ni(2)–S(12)	166.3 (1)
S(7)–Ni(2)–S(11)	96.1 (1)	S(10)–Ni(2)–S(12)	96.4 (1)
S(8)–Ni(2)–S(11)	165.1 (1)	S(11)–Ni(2)–S(12)	73.2 (1)

[a] Numbers in parentheses are estimated standard deviations in the least significant digits.

The NiS_6 coordination polyhedra show large distortions from octahedral geometry, much of which originate from the acute chelate bite angles. The polyhedra have approximate 3-fold symmetry, the deviations being more pronounced in molecule 1. In this molecule, the angles in the triangles (trigonal faces) $\Delta(S(1)S(3)S(5))$ and $\Delta(S(2)S(4)S(6))$ lie within the range 60 ± 2.4°; the angle subtended by the centroids of $\Delta(S(1)S(3)S(5))$ and $\Delta(S(2)S(4)S(6))$ at Ni(1) is 176.2°, and the centroid of the six sulfur atoms is virtually coincident with Ni(1) (distance 0.041 Å). In molecule 2, the trigonal faces are $\Delta(S(7)S(9)S(11))$ and $\Delta(S(8)S(10)S(12))$ and the corresponding parameters are 60 ±

(11) (a) Coucouvanis, D.; Fackler, J. P., Jr. *Inorg. Chem.* **1967**, *6*, 2047–2053. (b) Mohammed, T. J.; Mustafa, I. A.; Al-Mukhtar, S. E. *J. Indian Chem. Soc.* **1985**, *62*, 725–728.

(12) (a) Watt, G. W.; McCormick, B. J. *J. Inorg. Nucl. Chem.* **1965**, *27*, 898–900. (b) Fackler, J. P., Jr.; Schussler, D. P.; Chen, H. W. *Synth. React. Inorg. Met.-Org. Chem.* **1978**, *8*, 27–42. (c) Kruger, A. G.; Winter, G. *Aust. J. Chem.* **1972**, *25*, 2497–2501.

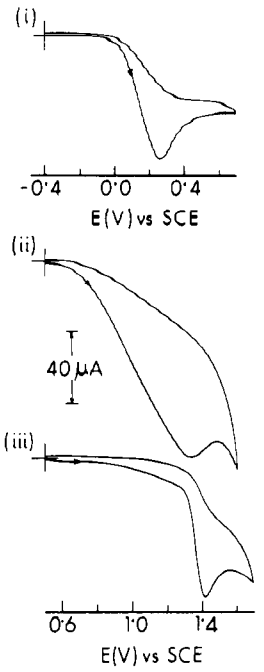

Figure 3. Cyclic voltammograms (scan rate 50 mV s^{-1}) of $\sim 10^{-3}$ M solutions of (i) KEtx, (ii) $Zn(Etx)_2$, and (iii) $Co(Etx)_3$ in acetonitrile (0.1 M TEAP) at a platinum electrode (298 K).

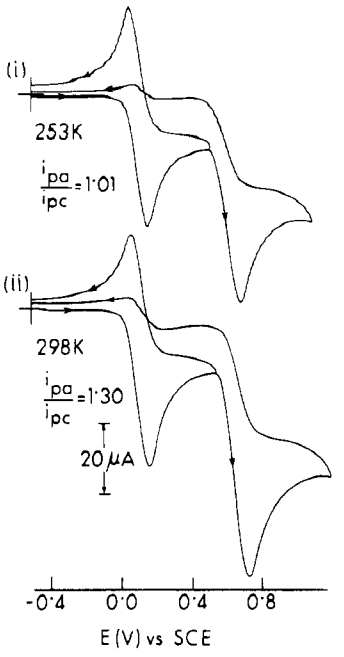

Figure 4. Cyclic voltammgrams (scan rate 50 mV s^{-1}) of $\sim 10^{-3}$ M solutions of $[Et_4N][Ni(Etx)_3]$ in acetonitrile (0.1 M TEAP) at a platinum electrode at (i) 253 K and (ii) 298 K.

1.3°, 179.9°, and 0.022 Å, respectively. The average trigonal twist angles in the two molecules are respectively 41.7 and 42.7°. Intermolecular S···S contacts are uniformly longer than 5.7 Å with one exception, viz. S(5)···S(10) = 3.798(2) Å. This contact is shown by dotted lines in Figure 2.

The structure of $[Me_3PhN][Ni(Etx)_3]$ has been referred to in the literature,[13] but neither the accuracy of the determination nor any other details (average Ni-S length is quoted[13a] to be 2.41 Å) are known to us. The average Ni-S distance in our complex is 2.439 (2) Å, which agrees well with the predicted sum of ionic radii[14] as well as with Ni-S distances in several paramagnetic octahedral complexes,[15] including a few containing xanthate ligands.[16] The corresponding distance in planar bis complexes of the type $Ni(Rx)_2$ is significantly shorter (2.21 Å).[16,17] The C-O and C-S distances in $Ni(Etx)_3^-$ are unexceptional for xanthate complexes.[16-19] The $Ni(Etx)_3^-$ ion, like[3b] $Ni(PhCS_2)_3^-$, is a rare example of a structurally characterized *anionic* $Ni^{II}S_6$ coordination sphere. Most reported structures of NiS_6 spheres pertain to cationic thioether complexes.[20] The average Ni-S distance in the latter lies in the range 2.39-2.43 Å.

B. Electrochemistry. All measurements were performed in acetonitrile solution (0.1 M in tetraethylammonium perchlorate) with platinum as the working electrode, and the potentials are referenced to the saturated calomel electrode (SCE). Potassium(I), zinc(II), and cobalt(III) salts of Rx^- were employed as controls for determining the nature of the redox process in $Ni(Rx)_3^-$. The electroactivity of a solution containing $Ni(Etx)_2$ and Etx^- has been mentioned in an earlier work.[5a]

a. Ligand Oxidation. The cyclic voltammograms of potassium xanthates consist of an anodic response near 0.3 V, but no cathodic peak is observed on scan reversal (Figure 3, Table I). Exhaustive constant-potential electrolysis at 0.5 V shows that the anodic response has one-electron stoichiometry. The disulfide EtOC(S)SS(S)COEt (Et_2x_2) was isolated from the oxidized solution in the case of R = Et. Iodine oxidation of potassium ethyl xanthate is known[21] to afford Et_2x_2. The electrochemical results can be rationalized in terms of the electrode reaction (eq 2) followed by rapid dimerization of the xanthate radical (eq 3). The dimerization process is virtually irreversible; vide infra.

$$ROC(S)S^\bullet + e \overset{E^\circ(2)}{\rightleftharpoons} ROC(S)S^- \quad (2)$$

$$2ROC(S)S^\bullet \overset{K(3)}{\rightleftharpoons} ROC(S)SS(S)COR \quad (3)$$

Ligand oxidation expectedly shows large anodic shifts upon chelation to cations as in $Zn(Rx)_2$ and $Co(Rx)_3$ (Figure 3). Selected anodic peak potential data (298 K): $Zn(Etx)_2$, 1.34 V; $Zn(n\text{-}Bux)_2$, 1.35 V; $Co(Etx)_3$, 1.43 V; $Co(n\text{-}Prx)_3$, 1.43 V. The exact nature of the ligand oxidation process in such complexes could be quite complex (as in related systems[22]) and does not concern us here.

b. Behavior of $Ni(Rx)_3^-$. Since metal-sulfur interaction is anticipated to be stronger in $Co(Rx)_3$ (trivalent metal) than in $Ni(Rx)_3^-$ (bivalent metal), ligand oxidation in the latter may be expected to occur at a potential lower than 1.40 V. But the potential should still lie far above that of solvated Rx^- ($\sim$0.3 V). When the voltage scan is limited to the range ±0.5 V, $Ni(Rx)_3^-$ displays a quasi-reversible cyclic response near 0.10 V with a peak-to-peak separation of 70-100 mV. (Figure 4, Table I). Clearly, this response cannot be due to ligand oxidation.

At 298 K anodic (i_{pa}) and cathodic (i_{pc}) peak currents are unequal, with i_{pa}/i_{pc} = 1.30 at a scan rate of 50 mV s^{-1} (R = Et).

(13) (a) Work of D'Addario, A.; Holah, D.; Knox, K. Quoted as a private communication in ref 15 of: Avdeef, A.; Fackler, J. P., Jr.; Fischer, R. G., Jr. *J. Am. Chem. Soc.* **1970**, *92*, 6972-6974. (b) Fackler, J. P., Jr.; Niera, R. D.; Canipana, C.; Trzcinoka-Bancroft, B. *J. Am. Chem. Soc.* **1984**, *106*, 7883-7886.
(14) Murray, S. G.; Hartley, F. R. *Chem. Rev.* **1981**, *81*, 365-414.
(15) (a) Udupa, M. R.; Krebs, B. *Inorg. Chim. Acta* **1981**, *52*, 215-218. (b) Hill, N. L.; Hope, H. *Inorg. Chem.* **1974**, *13*, 2079-2082.
(16) (a) Bizilz, K.; Hardin, S. G.; Hoskins, B. F.; Oliver, P. J.; Tiekink, E. R. T.; Winter, G. *Aust. J. Chem.* **1986**, *39*, 1035-1042. (b) Edwards, A. J.; Hoskins, B. F.; Winter, G. *Aust. J. Chem.* **1986**, *39*, 1983-1991. (c) Gable, R. W.; Hoskins, B. F.; Winter, G. *Inorg. Chim. Acta* **1985**, *96*, 151-159.
(17) (a) Chen, H. W.; Fackler, J. P., Jr. *Inorg. Chem.* **1978**, *17*, 22-26. (b) Hoskins, B. F.; Tiekink, E. R. T.; Winter, G. *Z. Kristallogr.* **1985**, *172*. 257-261.
(18) (a) Tiekink, E. R. T. *Z. Kristallogr.* **1987**, *181*, 251-255. (b) Snow, M. R.; Tiekink, E. R. T. *Aust. J. Chem.* **1987**, *40*, 743-750. (c) Tiekink, E. R. T.; Winter, G. *Aust. J. Chem.* **1986**, *39*, 813-816.
(19) Merlino, S. *Acta Crystallogr.* **1969**, *B25*, 2270-2276.
(20) (a) Setzer, W. N.; Ogle, C. A.; Wilson, G. S.; Glass, R. S. *Inorg. Chem.* **1983**, *22*, 266-271. (b) Cooper, S. R.; Rawle, S. C.; Hartman, J. A. R.; Hintsa, E. J.; Admans, G. A. *Inorg. Chem.* **1988**, *27*, 1209-1214. (c) Thorne, C. M.; Rawle, S. C.; Admans, G. A.; Cooper, S. R. *Inorg. Chem.* **1986**, *25*, 3848-3850.
(21) Reid, E. E. *Organic Chemistry of Bivalent Sulphur*; Chemical Publishing Co.: New York, 1962; Vol. 4.
(22) (a) Blankespoor, R. L. *Inorg. Chem.* **1985**, *24*, 1126-1128. (b) Bond, A. M.; Hollenkamp, A. F. *Inorg. Chem.* **1990**, *29*, 284-289.

Table III. Disproportionation Constants, $K(6)$ and $K(9)$, in Acetonitrile Solutions at 298 K[a]

soln no.[b]	10^3a_0,[c] M	b_0,[d] M	10^4c,[e] M	$K(6)$[f] or $K(9)$,[f] L mol^{-1}
1	5.414	1.004	2.586	398.7
2	8.314	1.210	4.048	380.6
3	11.745	1.202	5.623	392.8
4	2.250	0.207	1.260	58.7
5	3.676	0.236	2.137	61.8
6	4.970	0.243	3.037	57.3

[a] Meanings of $K(6)$ and $K(9)$ are as in text. [b] Solution numbers 1–3 and 4–6 correspond to xanthates and dithiocarbamates, respectively. [c] Initial concentrations of $Ni(Etx)_2$ or $Ni(Et_2d)_2$. [d] Initial concentrations of Et_2x_2 or Et_4d_2. [e] Equilibrium concentrations of $Ni(Etx)_3$ or $Ni(Et_2d)_3$. [f] Calculated by using eq 20.

In colder solutions (258 K) the two currents become equal within experimental error: $i_{pa}/i_{pc} = 1.01$. Upon constant-potential (0.35 V) coulometry at 258 K, the greenish yellow color of the original $Ni(Rx)_3^-$ solution changes to orange and the coulomb count for exhaustive electrolysis corresponds to one-electron oxidation (Table 1). The voltammogram (initial scan cathodic) of the oxidized solution is the same as that of the parent solution (initial scan anodic). The electrode reaction at ~0.1 V is assigned to oxidation of the metal center (eq 4). The EPR spectrum of the oxidized

$$Ni^{III}(Rx)_3 + e \overset{E°(4)}{\rightleftharpoons} Ni^{II}(Rx)_3^- \quad (4)$$

solution is consistent with this description of the oxidized complex. The formal potentials of the couple to eq 4 for the various complexes are listed in Table I.

When the voltage scan range on the positive side is increased, a second oxidiation is observed near 0.7 V (Figure 2). The i_{pa} of the new peak is approximately equal to that for the process of eq 4. Upon scan reversal only ill-defined cathodic peaks are observed even at 258 K (Figure 4). Since ligand oxidation in $Ni(Rx)_3$ (as in $Co(Rx)_3$) is expected to occur above 1 V, it is probable that the second anodic response is actually due to the formation of a nickel(IV) complex (eq 5), which decomposes rapidly. This process has not been investigated further.

$$Ni^{IV}(Rx)_3^+ + e \rightleftharpoons Ni^{III}(Rx)_3 \quad (5)$$

C. Disproportionation of $Ni(Rx)_3$ and Oxidative Addition of Disulfide to $Ni(Rx)_2$. The trivalent complex is thermally unstable. At 298 K it shows perceptible decomposition even on the cyclic voltammetric time scale, and this explains the $i_{pa}/i_{pc} > 1$ behavior of $Ni(Rx)_3^-$. At 258 K decomposition slows down and the current ratio becomes unity. Approximately 10^{-3} M solutions of $Ni(Rx)_3$ can be prepared by exhaustive electrolysis of corresponding solutions of $Ni(Rx)_3^-$ at 258 K or lower temperatures. The cold oxidized solutions can be preserved temporarily. Because of inherent instability, it has not been possible to isolate any $Ni(Rx)_3$ complex in pure state.

Upon warming of a cold orange solution of $Ni(Rx)_3$ to 298 K, its color rapidly changes and the resultant yellow solution is electrochemically silent in the voltage range ±0.5 V. It therefore does not contain significant concentrations of either $Ni(Rx)_3$ or $Ni(Rx)_3^-$. Actually, it contains $Ni(Rx)_2$ and the disulfide R_2x_2. This corresponds to metal reduction and oxidative dimerization of ligand. The reaction has been quantitatively studied for the case of R = Et.

A 2:1 mixture of $Ni(Etx)_2$ and Et_2x_2, prepared by codissolving the two compounds, has all properties identical with that of the decomposed solution originally containing an equivalent concentration of $Ni(Rx)_3$. The relationship between the three species is shown in eq 6. We have an equilibrium reaction shifted strongly

$$2Ni(Etx)_3 \overset{K(6)}{\rightleftharpoons} 2Ni(Etx)_2 + Et_2x_2 \quad (6)$$

$$K(6) = [Ni(Etx)_2]^2[Et_2x_2]/[Ni(Etx)_3]^2 \quad (7)$$

in the forward direction (disproportionation). When coulometrically synthesized $Ni(Etx)_3$ decomposes to the equilibrium level, little of it survives. On the other hand, observable concentrations of $Ni(Etx)_3$ can be generated by adding *excess* Et_2x_2 to $Ni(Etx)_2$. For a given concentration of $Ni(Etx)_2$, the concentration of $Ni(Etx)_3$ increases with increasing concentration of Et_2x_2 (Figure 5). Equilibium data determined voltammetrically (i_{pc} of the trivalent complex) are given in Table III. These are entirely consistent with EPR results reported later in this work.

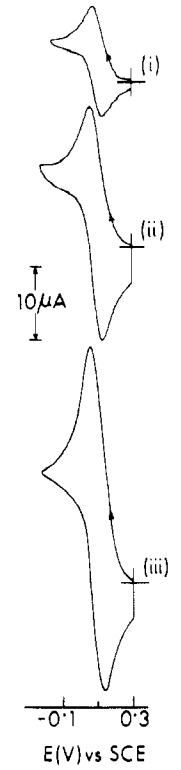

Figure 5. Cyclic voltammograms (scan rate 50 mV s^{-1}) of equilibriated solutions containing $Ni(Etx)_2$ and Et_2x_2 in acetonitrile (0.1 M TEAP) at a platinum electrode (298 K). Initial concentrations of $Ni(Etx)_2$, Et_2x_2: (i) 5.414×10^{-3}, 1.004 M; (ii) 8.314×10^{-3}, 1.210 M; (iii) 11.745×10^{-3}, 1.202 M.

The rate of the disulfide elimination reaction (forward reaction of eq 6) was followed by monitoring the cyclic voltammetric i_{pc} of $Ni(Etx)_3$ as a function of time. The rate process is strictly first order with respect to $Ni(Etx)_3$ (Figure 6). The rate constant at 253 K is 1.0×10^{-3} s^{-1}. Preliminary variable-temperature studies have afforded the following activation parameters: entropy, ~−40 eu; enthalpy, ~8 kcal mol^{-1}.

D. $Ni(Etx)_3$ in $Co(Etx)_3$ Lattice. Even though the isolation of $Ni(Etx)_3$ in pure solid form has not been feasible, the complex can be grown substitutionally in the crystal lattice of $Co(Etx)_3$. The strategy is to crystallize $Co(Etx)_3$ from solutions containing $Ni(Etx)_2$ and excess Et_2x_2 so as to ensure a significant equilibrium concentration of $Ni(Etx)_3$. One mole percent incorporation of $Ni(Etx)_3$ into $Co(Etx)_3$ crystals is easily achieved in this manner. The choice of the cobalt(III) complex as the host lattice was dictated by two factors. Its structure is accurately known,[19] and it is diamagnetic (low spin d^6). This ensured that the EPR technique could be meaningfully utilized for studying the nature of nickel(III) incorporation.

The unit cell and crystal system of a nickel(III)-doped (~1 mol %) single crystal of $Co(Etx)_3$ were determined by single-crystal X-ray diffractometry. The results are as follows: $a = 9.658$ (3) Å, $\alpha = 100.71$ (2)°, $V = 846.9$ (7) Å^3 (rhombohedral constraints). These agree, within experimental error, with those[19] of the pure $Co(Etx)_3$ lattice. EPR spectra of the nickel(III)-incorporated lattice is in agreement with isomorphous substitution of cobalt(III) by nickel(III).

E. EPR Spectra of $Ni(Rx)_3$. a. Frozen Glass. Solution spectra of $Ni(Rx)_3$ produced by electrochemistry or by mixing $Ni(Rx)_2$ and R_2x_2 were run as a frozen glass (77 K) (acetonitrile–toluene (1:1)) at X-band frequency. Representative results are shown

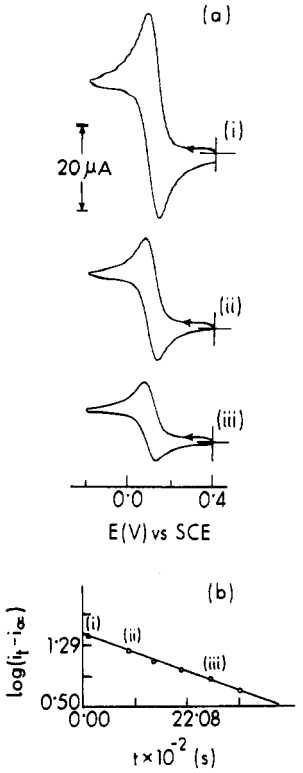

Figure 6. (a) Variable-time cyclic voltammograms (scan rate 50 mV s^{-1}) of electrogenerated $Ni(Etx)_3$ (initial concentration 1.226×10^{-3} M) at time (i) 2 min, (ii) 17 min, and (iii) 47 min in acetonitrile (0.1 M TEAP) at a platinum electrode at 253 K. (b) Plot of log $(i_t - i_\infty)$ vs time at 253 K.

Table IV. EPR g Values for $Ni(Rx)_3$[a]

R	g_1	g_2	g_3
Me	2.141	2.123	2.033
Et	2.141	2.124	2.035
	2.099[b]	2.099[b]	2.082[b]
n-Pr	2.140	2.124	2.035
i-Pr	2.140	2.124	2.038
n-Bu	2.143	2.123	2.033
i-Bu	2.141	2.124	2.035
s-Bu	2.140	2.122	2.034

[a] Unless otherwise stated, the spectra are in acetonitrile–toluene (1:1) glass (77 K). [b] Polycrystalline spectrum of $Ni(Etx)_3$ doped into a cobalt lattice at 77 K.

in Figure 7 and Table IV. The spectra are rhombic and are assigned to low-spin trivalent nickel (d^7, $S = {}^1/_2$) in a pseudooctahedral environment. The signal at highest field (g_3) is well separated from the other two (g_1 and g_2), which overlap with each other. The frozen complexes are thus pseudoaxial with the assignments $g_\parallel = g_3$ and $g_\perp = {}^1/_2(g_1 + g_2)$.

b. $Ni(Etx)_3$ in $Co(Etx)_3$. The polycrystalline spectrum of $Ni(Etx)_3$ in $Co(Etx)_3$ was examined at 77 K. It is significantly different from that in frozen glass (Figure 6). It is axial with $g_\perp = 2.099$ and $g_\parallel = 2.082$. These g values are respectively larger and smaller than frozen solution g_3 (2.035) and the average (2.136) of g_1 and g_2. On the other hand, the center of gravity (2.100) of frozen-solution signals lies very close to that (2.093) of the polycrystalline signals.

c. Correlation of Electrochemical and EPR Results. When equilibriated (298 K) solutions containing $Ni(Etx)_2$ and Et_2x_2 are rapidly cooled to 77 K, the population of $Ni(Etx)_3$ in the glassy state become frozen at the equilibrium level. The intensity of the nickel(III) EPR signals change in the expected manner upon changing the composition of the equilibrium solution (Figure 8). The agreement is quantitative. The height (turnover to turnover) for the g_2 EPR signal of frozen (77 K) solutions varies linearly (Figure 8) with cyclic voltammetric current heights (i_{pc}) of the same solutions (298 K), and the line passes through the origin.

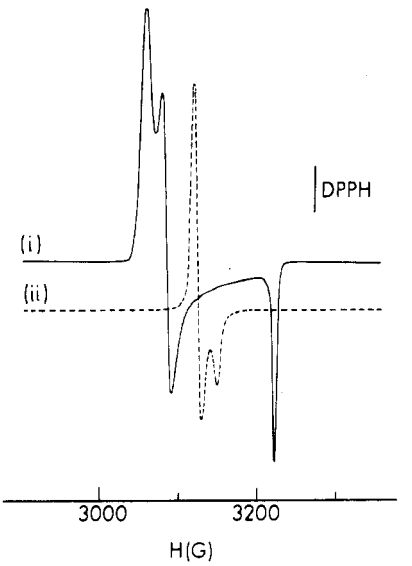

Figure 7. X-Band (9.119 GHz) 77 K EPR spectra of (i) electrogenerated $Ni(Mex)_3$ in 1:1 acetonitrile–toluene (—) and (ii) $Ni(Etx)_3$ doped into $Co(Etx)_3$ in polycrystalline form (---).

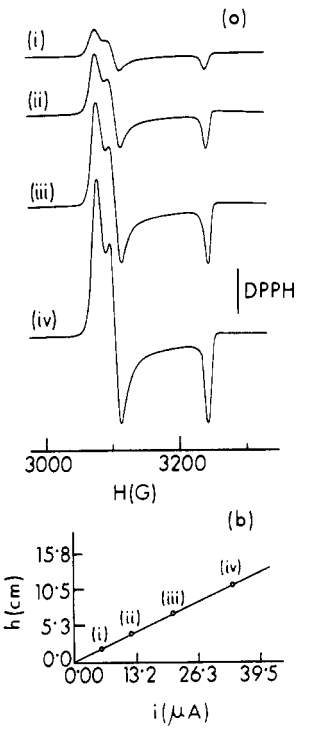

Figure 8. (a) X-Band (9.110 GHz) 77 K EPR spectra of equilibriated solutions (298 K) containing $Ni(Etx)_2$ and Et_2x_2 in 1:1 acetonitrile–toluene. Initial concentrations of $Ni(Etx)_2$, Et_2x_2: (i) 2.487×10^{-3}, 0.997 M; (ii) 5.946×10^{-3}, 1.016 M; (iii) 9.777×10^{-3}, 0.999 M; (iv) 1.875×10^{-2}, 0.402 M. (b) Plot of the heights (h) of the g_2 signals vs cyclic voltammetric current heights (i_{pc}).

The EPR results are thus in complete agreement with voltammetric equilibrium data of Table II.

F. Equilibria in Dithiocarbamato Complexes. The nickel(III) chemistry of dithiocarbamates[5] $R_2NC(S)S^-$ (abbreviated R_2d^-) is a qualitative parallel to that of Rx^-. On the quantitative plane, there are pronounced differences, some of which are quantitated here.

For the bivalent metal, the equilibrium of eq 8 is observed in solution.[5a] We have determined $K(8)$ using voltammetric methods.

$$Ni(Et_2d)_2 + Et_2d^- \overset{K(8)}{\rightleftharpoons} Ni(Et_2d)_3^- \qquad (8)$$

For solubility reasons a 3:2 acetonitrile–acetone mixture (instead of pure acetonitrile used for xanthates) is used as solvent. The average value of $K(8)$ at 298 K is 49 L mol^{-1}, which is at least

3 orders of magnitude smaller than $K(1)$ (>10^5 L mol^{-1}). Unlike the case of $Ni(Rx)_3^-$, it has not been possible to isolate any $Ni(R_2d)_3^-$ chelate as a salt so far. In the equilibrium of eq 9, Et_4d_2

$$2Ni(Et_2d)_3 \overset{K(9)}{\rightleftharpoons} 2Ni(Et_2d)_2 + Et_4d_2 \qquad (9)$$

is $Et_2NC(S)SS(S)CNEt_2$. From voltammetry the average value of $K(9)$ at 298 K is found to be 59 L mol^{-1} (Table III). This is less than one-sixth of $K(6)$ (391 L mol^{-1}). Thus, disproportionation is much less prevelant in $Ni(Et_2d)_3$. A linear relationship between voltammetric current height and EPR signal height entirely analogous to that of the xanthate system (Figure 8) applies here as well.

Our results (298 K) on the reduction potentials of couples of eq 10 (−0.29 V) and eq 11 (−0.01 V) agree with literature data.[5a,23]

$$Ni(Et_2d)_3 + e \overset{E°(10)}{\rightleftharpoons} Ni(Et_2d)_3^- \qquad (10)$$

$$Et_2d^{\bullet} + e \overset{E°(11)}{\rightleftharpoons} Et_2d^- \qquad (11)$$

The reduction in eq 10 is followed by dissociation (eq 8) and oxidation of eq 11 is followed by rapid dimerization (eq 12). The

$$2Et_2d^{\bullet} \overset{K(12)}{\rightleftharpoons} Et_4d_2 \qquad (12)$$

reduction potential of the couple of eq 10 is taken as the average of anodic and cathodic peak potentials, and that of the couple of eq 11 is calculated from anodic peak potential by subtracting 30 mV.

Discussion

A. Coordination Geometry and EPR Spectra of $Ni(Rx)_3$. Bidentate chelation by the Rx^- units is expected to afford an S_6 coordination sphere for nickel(III) in $Ni(Rx)_3$. The following three observations taken collectively ensure that this is indeed so: (i) the S_6 sphere of $Ni(Rx)_3^-$ precursors, proved in one case (R = Et) by structure determination, (ii) facile electrochemical interconversion of $Ni(Rx)_3$ and $Ni(Rx)_3^-$, suggesting absence of major structural changes during metal redox, and (iii) substitutional incorporation of $Ni(Etx)_3$ into the lattice of $Co(Etx)_3$, which definitely has[19] CoS_6 coordination.

In the $Co(Etx)_3$ lattice, strict 3-fold symmetry is crystallographically imposed with the cobalt atom lying at a special position (0.2934 (2), x, x) in the rhombohedal space group $R\bar{3}$.[19] The axial EPR spectrum of $Ni(Etx)_3$ in the $Co(Etx)_3$ lattice is thus entirely consistent with substitutional occupation of cobalt(III) sites by nickel(III). In idealized D_{3d} symmetry, the octahedral t_{2g} and e_g orbitals are transformed into $a_{1g} + e_g$ and e_g, respectively. In this symmetry, the electronic configuration of $Ni(Etx)_3$ is $(a_{1g}, e_g)^6(e_g)^1$. Being an orbital doublet with an unpaired electron in an antibonding level, this configuration is subject to Jahn–Teller distortion. In the $Co(Etx)_3$ lattice, the anticipated distortion remains unexpressed due no doubt to the crystallographic symmetry constraint. In frozen glass solution, no such constraint is operative and the spectrum now shows the expected Jahn–Teller splitting into rhombic components (Figure 7). The precise nature of the distortion is unknown, but inequalization of metal–ligand distances is a good possibility, as observed in certain NiN_6 chelates.[24,25] A variable-temperature EPR study of $Ni(Etx)_3$ is in progress.

B. Nickel(III)–Sulfur Binding. A coordinate covalent bond of type L→M involves a net transfer of negative charge from ligand to metal.[1a,1f,26] In most cases this does not vitiate the oxidation-state description of the metal ion. Such is the situation for nickel(III) in a plethora of environments with nitrogen as the commonest donor atom.[1,2] In the environment of easily polarizable ligands, the charge-transfer process may proceed too far, leading to ligand oxidation and metal reduction. A suggestion has indeed been made[7b] that one-electron oxidation of the nickel(II)–thiolato function affords the nickel(II)–thiyl moiety **3a** with ligand and

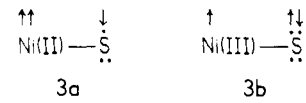

metal unpaired electrons antiferromagnetically coupled ($S = {}^1/_2$). Viewed against the nickel(III)–thiolato description **3b**, this model corresponds to an extreme level of ligand-to-metal charge transfer.

There are no constraints that disallow configurations intermediate between **3a** and **3b**, and we propose that such resonance hybrids could provide a general and rational qualitative description of the binding of sulfur ligands to nickel(III). The cannonical form **3a** may then approximate the activated state for the reaction (eq 13) that eventually leads to disulfide formation following

$$NiS- \rightarrow [\mathbf{3a}] \rightarrow Ni(II) + -S-S- \qquad (13)$$

radical elimination. The closer the hybrid is to **3a**, the more facile should be the reaction of eq 13. There are instances[27] where disulfide formation occurs immediately upon oxidation of nickel(II) thiolates. These are good candidates for the extreme situation where the oxidized complex is itself very much like **3a**. In other instances[7b] detectable oxidized complexes with anisotropic **g** tensors are first formed, which subsequently afford disulfide. Here the resonance hybrid description with substantive contribution from **3b** is appropriate.

The $Ni(Rx)_3$ species occupy a most interesting position in this model. Here an electron is reversibly transferable between xanthate and nickel(III). The net result is the solution equilibrium of eq 6. The ground state of $Ni(Rx)_3$ is believed to be a resonance hybrid of bonding types **3a** and **3b** with a large contribution from **3b**.

C. Reactivity of $Ni(Rx)_3$. Perfectly stable concentrations of $Ni(Rx)_3$ can be generated in solution in accordance with the disproportionation equilibrium, eq 6. Instability arises only when populations are in excess of equilibrium values, as in electrosynthesis from $Ni(Rx)_3^-$. Such solutions can still be stored, but only temporarily in cold condition (slow decomposition). Molecular mobility plays a crucial role in destabilizing $Ni(Rx)_3$. Once mobility is arrested, $Ni(Rx)_3$ becomes indefinitely stable even at 300 K, as in the case of $Ni(Etx)_3$ in the $Co(Etx)_3$ lattice.

The observed first-order dependence of the disproportionation rate on $Ni(Etx)_3$ is consistent with a rate-determining step as in eq 14. The fast dimerization of the Etx$^{\bullet}$ radical may proceed

$$Ni(Etx)_3 \xrightarrow{rds} Ni(Etx)_2 + Etx^{\bullet} \qquad (14)$$

$$Etx^{\bullet} + Ni(Etx)_3 \xrightarrow{fast} Ni(Etx)_2 + Et_2x_2 \qquad (15)$$

either as in eq 3 or by collision with a second $Ni(Etx)_3$ molecule as in eq 15. Molecular mobility is evidently needed for dimerization to materialize. The large negative entropy of activation (~−40 eu) of the disproportionation reaction can be attributed at least in part to the localization and ordering involved in the traverse from the ground state (a hybrid of **3a** and **3b** with large **3b** weightage) to a **3a**-like transition state such as $Ni^{II}(Etx)_2(Etx^{\bullet})$, in which the radical is still attached to the metal.

In the reaction of eq 15, a transient metal-bound disulfide species can be a rational intermediate. The slow (eq 16) backward

$$k_b(6) = k_f(6)/K(6) \approx 2.60 \times 10^{-6}\ s^{-1} \qquad (16)$$

reaction of eq 6 can then proceed via the same intermediate. Disulfide-coordinated nickel(II) species are known.[7b] Metal coordination usually weakens the disulfide bond, favoring homolytic cleavage.[28]

(23) Scrimager, C.; Dehayes, L. J. *Inorg. Nucl. Chem. Lett.* **1978**, *14*, 125–133.
(24) Wieghardt, K.; Walz, W.; Nuber, B.; Weiss, J.; Ozarowski, A.; Stratemeire, H.; Reinen, D. *Inorg. Chem.* **1986**, *25*, 1650–1654.
(25) Szalda, D. J.; Macartney, D. H.; Sutin, N. *Inorg. Chem.* **1984**, *23*, 3473–3479.
(26) Nyholm, R. S.; Tobe, M. L. *Adv. Inorg. Chem. Radiochem.* **1963**, *5*, 1–40.
(27) Krüger, H.-J.; Holm, R. H. *Inorg. Chem.* **1989**, *28*, 1148–1155.

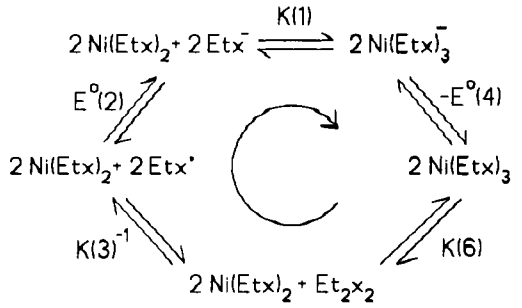

Figure 9. Cycle of the equilibria.

D. Free Energy Cycle. a. Factors Favoring Trivalent Nickel. The processes of eq 1–4 and 6 can be combined into the cycle of Figure 9. The sign and indices (±1) of the thermodynamic constants shown in the figure correspond to a clockwise traverse of the cycle. For the full cycle, the relationship of eq 17 is valid.

$$2F(E^\circ_T(4) - E^\circ_T(2)) - RT \ln (K^2(1)\, K(6)/K(3)) = 0 \quad (17)$$

$$2F(E^\circ_T(10) - E^\circ_T(11)) - RT \ln (K^2(8)\, K(9)/K(12)) = 0 \quad (18)$$

For a similar cycle, eq 18 can be derived for the dithiocarbamate system. At 298 K, experimental quantities for R = Et are as follows: $K(1) = 10^5$ L mol^{-1}, $E^\circ(2) = -0.23$ V, $E^\circ(4) = 0.11$ V, $K(6) = 391$ L mol^{-1}; $K(8) = 49$ L mol^{-1}, $K(9) = 59$ L mol^{-1}, $E^\circ(10) = -0.29$ V, $E^\circ(11) = -0.01$ V. The only unknown quantities are $K(3)$ and $K(12)$. Their values are found to be 4.56×10^{16} L mol^{-1} and 4.38×10^{14} L mol^{-1}, respectively.

The greater stability of the $Et_2d^\bullet$ radical compared to the $Etx^\bullet$ radical is consistent with the greater electron density on sulfur atoms in Et_2d^- compared to Etx^- (larger contribution of structure **4b** in the case of dithiocarbamates[29]). The $Etx^\bullet$ and $Et_2d^\bullet$ di-

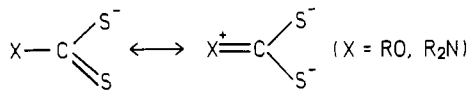

4a 4b

merization constants are larger than that of an aryl thiyl,[30] which may be subject to stabilization through aromatic delocalization.

Using the cycles, one can analyze the factors that favor the trivalent complex with respect to the disproportionation reactions of eq 6 and 9. Stability of the complex increases as (i) the radical dimerization constant becomes smaller, (ii) the nickel(III)–nickel(II) reduction potential decreases, (iii) the stability of the nickel(II) tris chelate increases, and (iv) the redox potential of the ligand becomes more positive. The free energy differences between Rx^- and R_2d^- systems corresponding to these four factors are collected in Table V. The $Ni(Et_2d)_3$ complex is favored ($K(6) > K(9)$) over $Ni(Etx)_3$ by the factors i and ii, the latter being particularly dominant. Factors of types iii and iv are unfavorably disposed for $Ni(Et_2d)_3$, but their net effect falls short of (i) + (ii).

Factors i–iv can all be related to the negative charge of sulfur atoms in Etx^- and Et_2d^-. The inequality $K(3) > K(12)$ has already been examined from this angle. The relations $E^\circ(4) > E^\circ(10)$ and $E^\circ(2) > E^\circ(11)$ are as expected (smaller charge density in Etx^-). Since R_2d^- has a larger charge density, the inequality $K(1) \gg K(8)$ is apparently paradoxical. Evidently, the strong donor ability of Et_2d^- leads to sufficient metal-to-ligand charge transfer at the bis complex stage itself and $Ni(R_2d)_2$ has only weak affinity for a third anionic ligand. On the other hand, three molecules of the weaker Etx^- donor can conveniently bind to one nickel(II) ion. Unlike the case of the bivalent species, there is no evidence of nonoxidative ligand dissociation from either $Ni(Etx)_3$ or $Ni(Et_2d)_3$, evidently due to increased metal charge with a larger demand for donor electron density.

Table V. Free Energy Differences of Xanthate and Dithiocarbamate Equilibria

process[a]	free energy diff, kcal mol^{-1}
radical dimerizn (eqs 3 and 12)	$(\Delta G^\circ(3) - \Delta G^\circ(12)) = -2.6$[b]
tris nickel(III)–nickel(II) redox (eqs 4 and 10)	$(\Delta G^\circ(4) - \Delta G^\circ(10)) = -18.5$[c]
bis–tris equilibria of nickel(II) (eqs 1 and 8)	$-(\Delta G^\circ(1) - \Delta G^\circ(8)) = 9.0$[c]
ligand redox (eqs 2 and 11)	$-(\Delta G^\circ(2) - \Delta G^\circ(11)) = 11.0$[c]
disproportionation (eqs 6 and 9)	$(\Delta G^\circ(6) - \Delta G^\circ(9)) = -1.1$[c]

[a] Equation numbers are as in text. [b] Derived from the thermodynamic cycle. [c] Derived experimentally.

b. Bioinorganic Implications. The above analysis throws significant light on some aspects of nickel(III) in hydrogenases.[9,10] The immediate one is that the sulfur-bonded nickel(III)–nickel(II) reduction potential has to be low and will therefore be suitable for executing reduction rather than oxidation of substrates. This follows from the fact that, other things remaining the same, the disproportionation of the Ni(III)–S system is most effectively hindered by lowering the nickel(III)–nickel(II) reduction potential (Table V).

In fluid media containing sulfur donor centers in the oxidation states −2 (sulfide, thiol, thioether) and 0 (thiyl, disulfide), bivalent and/or trivalent states of nickel can exist as a natural thermodynamic consequence of ligational and redox equilibria. The balance of free energy changes dictates the relative abundance of the metal oxidation states. Evidently, such abundance would be subject to chemical control through ligands or groups (attached to nickel and sulfur) that can influence the above mentioned equilibria. Viewed from this angle, the occurrence of the +3 oxidation state of nickel in living cells where thiol and disulfide functions are available is not unexpected.

The frozen-solution EPR spectrum of $Ni(Etx)_3$ quanlitatively resembles those of nickel(III) hydrogenases.[31] The spectra are rhombic with the $g_\perp$ components standing distinctly apart from $g_\parallel$. The magnitudes of the $g_\perp$ components are larger in the hydrogenases, and the $g_\perp$ splittings are also greater. However, in both cases, we have $g_\perp > g_\parallel$, which signifies a $d^1_{z^2}$ ground state.[1a] Unfortunately, this result does not reveal the composition of the coordination sphere in hydrogenases, since the majority of pseudooctahedral nickel(III) complexes abide by the $g_\perp > g_\parallel$ rule.[1]

E. Concluding Remarks. The main results and conclusions of this research will be summarized. A tris(xanthate) of nickel(II), $Ni(Etx)_3^-$, has been structurally characterized, revealing the presence of nearly axial anionic NiS_6 coordination spheres. Chelates of this type are in general quantitatively electrooxidizable near 0.1 V to $Ni(Rx)_3$. The latter (R = Et) has been substitutionally incorporated into the lattice of $Co(Etx)_3$, and in this condition the 77 K EPR spectrum ($S = {}^1/_2$) of $Ni(Etx)_3$ is axial due to the dictates of crystal symmetry. The expected Jahn–Teller distortion becomes observable once crystal constraints are removed, as in 77 K frozen glass.

The nickel(III) description of $Ni(RX)_3$ is appropriate, possibly with some resonance contribution from a structure of type $Ni^{II}(Etx)_2(Etx^\bullet)$. Localization into the latter form is a probable pathway for the first-order disproportionation of $Ni(Rx)_3$ into $Ni(Rx)_2$ and R_2x_2.

The last three species constitute a remarkable chemically reversible redox system characterized by ligand-to-metal electron transfer in one direction (disproportionation) and oxidative addition of the disulfide moiety to nickel(II) in the other direction. Dithiocarbamates display a cognate behavior, and the relative redox status of the xanthate and the dithiocarbamate systems find ra-

(28) (a) Kuehn, C. G.; Isied, S. S. *Prog. Inorg. Chem.* **1980**, *27*, 153–221. (b) Treichel, P. M.; Rosenhein, L. D.; Schmidt, M. S. *Inorg. Chem.* **1983**, *22*, 3960–3965.
(29) Coucouvanis, D. *Prog. Inorg. Chem.* **1970**, *11*, 233–371.
(30) Griller, D.; Barclay, L. R. C.; Ingold, K. U. *J. Am. Chem. Soc.* **1975**, *97*, 6151–6154.
(31) (a) Cammack, R.; Patil, D.; Aguirre, R.; Hatchikian, E. C. *FEBS Lett.* **1982**, *142*, 289–292. (b) Albracht, S. P. J.; Graf, E.-G.; Thauer, R. K. *FEBS Lett.* **1982**, *140*, 311–313. (c) Kojima, N.; Fox, J. A.; Hausinger, R. P.; Daniels, L.; Orme-Johnson, W. H.; Walsh, C. *Proc. Natl. Acad. Sci. U.S.A.* **1983**, *80*, 378–382.

tionalization in terms of sulfur nucleophilicity ($Rx^- < R_2d^-$).

In solutions containing sulfur donor centers in oxidation states −2 and 0, the bivalent and/or trivalent states of nickel appear as natural thermodynamic entities. For hindering disproportionation of the $Ni^{III}S$ fragment, it is mandatory to have low nickel(III)–nickel(II) reduction potential in sulfur-coordinated systems. These observations are evidently significant with respect to nickel(III) in hydrogenases. At present, we are scrutinizing the redox chemistry of several other nickel–sulfur systems.

Experimental Section

Physical Measurements. Microanalytical data (C, H, N) were obtained with a Perkin-Elmer Model 240C elemental analyzer. Electronic spectra were recorded with a Hitachi 330 spectrophotometer. EPR spectra were recorded in the X-band on a Varian E-109C spectrometer fitted with a quartz Dewar flask for measurements at 77 K (liquid nitrogen). The spectra were calibrated with respect to DPPH ($g = 2.0037$). Electrochemical measurements were done by using the PAR Model 370-4 electrochemistry system incorporating a Model 174 A polarographic analyzer, Model 175 universal programmer, Model RE0074 X-Y recorder, Model 173 potentiostat, Model 179 digital coulometer, and Model 377 cell system. A planar Beckman Model 39273 platinum-inlay working electrode, a platinum-wire auxiliary electrode, and an aqueous saturated calomel reference electrode (SCE) were used in three-electrode measurements. A platinum-wire-gauge working electrode was used in coulometric experiments. All experiments were performed under dinitrogen atmosphere, and reported potentials are uncorrected for junction contribution. Haake Model-F3K and Model-D8G digital cryostats and circulators connected to appropriate jacketed cells were used for low-temperature electrochemical measurements.

Preparation of Ligands and Complexes. Potassium xanthates (KRx),[11] diethyldixanthogen, (Et_2x_2),[21] bis complexes of zinc, $Zn(Rx)_2$,[27] tris complexes of cobalt, $Co(Rx)_3$,[12a] bis and tris complexes of nickel, $Ni(Rx)_2$[11] and $Ni(Rx)_3^-$[11] (isolated as their tetraethylammonium salts), were prepared by general literature methods. Some of the $Ni(Rx)_3^-$ species are new. Results of elemental analyses (C, H, N) for those are reported below.

Tetraethylammonium Tris(*n*-propyl xanthato)nickelate(II), [Et_4N][Ni(*n*-Prx)$_3$]. Anal. Calcd for $NiC_{20}H_{41}NO_3S_6$: C, 40.42; H, 6.91; N, 2.36. Found: C, 40.34; H, 6.73; N, 2.21.

Tetraethylammonium Tris(isopropyl xanthato)nickelate(II), [Et_4N][Ni(*i*-Prx)$_3$]. Anal. Calcd for $NiC_{20}H_{41}NO_3S_6$: C, 40.42; H, 6.91; N, 2.36. Found: C, 40.22; H, 6.61; N, 2.41.

Tetraethylammonium Tris(*n*-butyl xanthato)nickelate(II), [Et_4N][Ni(*n*-Bux)$_3$]. Anal. Calcd for $NiC_{23}H_{47}NO_3S_6$: C, 43.42; H, 7.40; N, 2.20. Found: C, 43.27; H, 7.33; N, 2.22.

Tetraethylammonium Tris(isobutyl xanthato)nickelate(II), [Et_4N][Ni(*i*-Bux)$_3$]. Anal. Calcd for $NiC_{23}H_{47}NO_3S_6$: C, 43.42; H, 7.40; N, 2.20. Found: C, 43.29; H, 7.24; N, 2.13.

Tetraethylammonium Tris(*sec*-butyl xanthato)nickelate(II), [Et_4N][Ni(*s*-Bux)$_3$]. Anal. Calcd for $NiC_{23}H_{47}NO_3S_6$: C, 43.42; H, 7.40; N, 2.20. Found: C, 43.31; H, 7.31; N, 2.24.

Tetraethylammonium Tris(methyl xanthato)nickelate(II), [Et_4N][Ni(Mex)$_3$]. Anal. Calcd for $NiC_{14}H_{29}NO_3S_6$: C, 32.96; H, 5.69; N, 2.75. Found: C, 32.78; H, 5.53; N, 2.49.

The dithiocarbamato complex $Ni(Et_2d)_2$ was prepared as reported.[11] Aldrich Chemical Et_4d_2 was used.

Determination of the Equilibrium Constant for the Bis–Tris Equilibrium (Eqs 1 and 8). $Ni(Etx)_2$ and KEtx were mixed in different molar concentrations in acetonitrile, and the intensity of the ligand field (ν_1) band of $Ni(Etx)_3^-$ at 1065 nm was monitored spectrophotometrically in thermostated cells (298 K). Neither $Ni(Etx)_2$ nor KEtx absorbs in this wavelength region. From the intensity of the ligand field band, the equilibrium concentrations of $Ni(Etx)_3^-$ were obtained. The extinction coefficient of $Ni(Etx)_3^-$ is 44.9 L mol^{-1} cm^{-1}. Equilibrium concentrations of $Ni(Etx)_2$ and Etx^- were determined from the reaction stoichiometry expressed in eq 1. The measurements showed that the forward reaction was virtually complete at all stages and only the lower limit of $K(1)$ could be set as 10^5 L mol^{-1}.

$Ni(Et_2d)_2$ and $NaEt_2d$ were mixed at 298 K in different molar concentrations in 3:2 acetonitrile–acetone, and the current height of the voltammetric response at −0.26 V due to $Ni(Et_2d)_3$ was monitored cyclic voltammetrically. The equilibrium concentrations of $Ni(Et_2d)_3$ were obtained from the current heights, and the equilibrium concentrations of $Ni(Et_2d)_2$ and $NaEt_2d$ were obtained from the reaction stoichiometry of eq 8. The initial concentrations of $Ni(Et_2d)_2$ and $NaEt_2d$ were varied in the ranges 3.5×10^{-4}–5.1×10^{-4} and 3.5×10^{-3}–4.3×10^{-3} M, respectively. The values (three measurements) of $K(8)$ spanned the range 47–52 L mol^{-1}, with an average of 49 L mol^{-1}.

Table VI. Crystallographic Data for [Et_4N][$Ni(Etx)_3$]

chem formula $C_{17}H_{35}NO_3S_6Ni$	$Z = 8$
fw 552.5	$T = 23 \pm 1$ °C
space group $P2_1/n$	$\lambda = 0.71073$ Å
$a = 18.842$ (7) Å	$\rho_{calcd} = 1.384$ g cm^{-3}
$b = 16.448$ (4) Å	$\mu = 12.05$ cm^{-1}
$c = 18.987$ (7) Å	transm coeff = 0.7631–0.7219
$\beta = 115.65$ (3)°	$R^a = 0.0484$
$V = 5304$ (2) Å^3	$R_w{}^b = 0.0578$

$^a R = \sum||F_o| - |F_c||/\sum|F_o|$. $^b R_w = [\sum w(|F_o| - |F_c|)^2/\sum w|F_o|^2]^{1/2}$; $w^{-1} = \sigma^2(|F_o|) + 0.0004|F_o|^2$.

Table VII. Atomic Coordinates (×10^4) and Equivalent Isotropic Displacement Coefficients (Å^2 × 10^3) (with Their Estimated Standard Deviations in Parentheses) for [Et_4N][$Ni(Etx)_3$]^a

atom	x	y	z	U(eq)
Ni(1)	6603 (1)	3861 (1)	2571 (1)	45 (1)
Ni(2)	7709 (1)	5931 (1)	6715 (1)	44 (1)
S(1)	6214 (1)	2934 (1)	3341 (1)	56 (1)
S(2)	6383 (1)	2536 (1)	1926 (1)	53 (1)
S(3)	5315 (1)	4503 (1)	1827 (1)	55 (1)
S(4)	6714 (1)	4673 (1)	1556 (1)	49 (1)
S(5)	7059 (1)	4958 (1)	3510 (1)	54 (1)
S(6)	8024 (1)	3672 (1)	3331 (1)	48 (1)
S(7)	8468 (1)	6070 (1)	8123 (1)	54 (1)
S(8)	8644 (1)	4799 (1)	7148 (1)	60 (1)
S(9)	6663 (1)	5128 (1)	6790 (1)	48 (1)
S(10)	6932 (1)	5398 (1)	5412 (1)	52 (1)
S(11)	7074 (1)	7264 (1)	6508 (1)	53 (1)
S(12)	8504 (1)	6859 (1)	6353 (1)	57 (1)
O(1)	6132 (3)	1465 (3)	2848 (3)	58 (2)
O(2)	5466 (2)	5525 (2)	809 (2)	52 (2)
O(3)	8622 (2)	4883 (3)	4268 (3)	57 (2)
O(4)	9441 (3)	4882 (3)	8694 (3)	72 (2)
O(5)	5828 (2)	4432 (3)	5477 (2)	48 (2)
O(6)	7966 (3)	8318 (3)	6186 (3)	59 (2)
N(1)	3304 (3)	2604 (3)	836 (3)	42 (2)
N(2)	9096 (3)	2370 (3)	1579 (3)	45 (2)
C(1)	6048 (5)	42 (4)	2645 (6)	98 (6)
C(2)	6235 (4)	816 (4)	2368 (4)	67 (4)
C(3)	6234 (3)	2241 (4)	2699 (3)	47 (3)
C(4)	4587 (4)	6628 (5)	216 (4)	82 (4)
C(5)	4684 (4)	5837 (4)	639 (4)	65 (3)
C(6)	5784 (3)	4949 (4)	1355 (3)	46 (3)
C(7)	9379 (5)	5822 (5)	5231 (5)	100 (5)
C(8)	8589 (4)	5640 (4)	4654 (4)	69 (4)
C(9)	7954 (3)	4544 (3)	3750 (3)	44 (3)
C(10)	10543 (5)	4036 (5)	9389 (4)	92 (4)
C(11)	9791 (4)	4100 (5)	8684 (5)	79 (4)
C(12)	8905 (3)	5204 (4)	8034 (4)	52 (3)
C(13)	5077 (4)	3508 (4)	4476 (4)	66 (3)
C(14)	5607 (4)	4222 (4)	4657 (3)	57 (3)
C(15)	6421 (3)	4950 (3)	5841 (3)	40 (2)
C(16)	7688 (6)	9703 (5)	5971 (6)	108 (6)
C(17)	7466 (4)	8954 (4)	6242 (5)	70 (4)
C(18)	7848 (3)	7556 (4)	6343 (3)	47 (3)
C(19)	2195 (4)	2101 (5)	1157 (4)	78 (4)
C(20)	2458 (4)	2685 (4)	714 (4)	62 (3)
C(21)	3030 (5)	3389 (5)	−413 (4)	95 (5)
C(22)	3504 (4)	3311 (4)	453 (4)	72 (4)
C(23)	3796 (4)	3308 (4)	2159 (4)	68 (3)
C(24)	3870 (4)	2610 (5)	1697 (4)	72 (3)
C(26)	3384 (4)	1813 (4)	488 (4)	68 (3)
C(25)	4196 (5)	1643 (6)	545 (5)	116 (5)
C(27)	10364 (4)	1531 (5)	2075 (5)	95 (5)
C(28)	9504 (4)	1585 (4)	1527 (4)	66 (3)
C(29)	9525 (5)	3118 (6)	654 (5)	98 (5)
C(30)	9489 (4)	3116 (4)	1427 (4)	61 (3)
C(31)	7729 (4)	3000 (5)	920 (5)	87 (4)
C(32)	8245 (3)	2294 (4)	966 (4)	62 (3)
C(33)	8721 (4)	1866 (4)	2647 (4)	68 (4)
C(34)	9138 (4)	2498 (4)	2390 (3)	52 (3)

^{a} Equivalent isotropic U defined as one-third of the trace of the orthogonalized U_{ij} tensor.

Electrosynthesis of $Ni(Rx)_3$ in Solution. The case of R = Et is cited here as an example of the general procedure used. A 20-mL acetonitrile

solution containing 11.87 mg (2.15×10^{-5} mol) of $(Et_4N)[Ni(Etx)_3]$ and 0.46 g (2.00 mmol) of TEAP was cooled to 253 K in the thermostatic coulometric cell. The potential of the platinum gauge working electrode was fixed at 0.35 V. The oxidation was completed at a count of 2.073 C (the calculated count for one-electron oxidation was 2.076 C). At this stage, nearly all the nickel in solution is present as $Ni(Etx)_3$.

Rate of Disproportionation of $Ni(Etx)_3$. Solutions of $Ni(Etx)_3$ prepared as above were allowed to decompose in a thermostatic cell. The concentration of $Ni(Etx)_3$ was monitored cyclic voltammetrically by recording the current heights as a function of time (t). The relevant rate equation is given by eq 19, where i_0, i_t, and i_∞ are the current heights (i_{pc} in microamperes) at $t = 0$, $t = t$, and $t = \infty$ (i.e., at equilibrium). Because of the equilibrium situation (eq 6), $i_\infty \neq 0$. The rate constant was obtained from a linear least-squares plot of $\log (i_t - i_\infty)$ against t. The rate constant was corrected for the back-reaction by using standard procedures[32] (the correction was small and amounted to ~3%).

$$-\log (i_t - i_\infty) = (k_f(6)\ t/2.303) - \log (i_0 - i_\infty) \qquad (19)$$

Determination of the Disproportionation Equilibrium Constant (Eqs 6 and 9). Acetonitrile solutions of $Ni(Etx)_2$ ($\sim 10^{-3}$–10^{-2} M) and Et_2x_2 (~1.0 M) were allowed to equilibrate in a thermostatic cell. Equilibrium was reached almost immediately. The concentrations of $Ni(Etx)_3$ produced at equilibrium were determined cyclic voltammetrically, and the equilibrium concentrations of $Ni(Etx)_2$ and Et_2x_2 were determined from reaction stoichiometry. The value of the equilibrium constant was determined by eq 20, where a_0, b_0, and c are initial concentration of $Ni(Etx)_2$, initial concentration of Et_2x_2, and equilibrium concentration of $Ni(Etx)_3$, respectively. The same method was applied for the determination of the disproportionation constant of $Ni(Et_2d)_3$. Only $Ni(Et_2d)_2$ and Et_4d_2 were used instead of $Ni(Etx)_2$ and Et_2d_2. Results are given in Table III.

$$K(6) = (a_0 - c)^2(b_0 - 0.5c)/c^2 \qquad (20)$$

Correlation of Voltammetric Current Height with EPR Signal Height. The same solutions as those used above were frozen quickly to 77 K, and EPR spectra were run. The signal heights of g_2 (turnover to turnover, in centimeters) were plotted against the corresponding voltammetric current heights (i_{pc} in microamperes), to produce a straight-line plot.

Doping of $Co(Etx)_3$ by $Ni(Etx)_3$. To a solution of $Ni(Etx)_2$ (29.88 mg, 9.94×10^{-5} mol) in 5 mL of dichloromethane was added 1.579 g (6.52×10^{-3} mol) of Et_2x_2. After this solution was kept for 3 h, 0.2 mL was then mixed well with a 20-mL dichloromethane solution of $Co(Etx)_3$ (65.69 mg, 1.56×10^{-4} mol). Green crystals of $Co(Etx)_3$ doped by $Ni(Etx)_3$ were obtained by slow evaporation of this solution. The crystals were then washed with methanol and dried in vacuo.

Determination of the Cell Dimensions of a $Co(Etx)_3$ Crystal Doped with $Ni(Etx)_3$. Single crystals of $Co(Etx)_3$ doped by $Ni(Etx)_3$ were grown as described above. A green prismatic crystal (0.32 mm × 0.24 mm × 0.28 mm) was chosen for the determination of its cell parameters. The unit cell parameters were determined by a least-squares fit of 20 machine-centered reflections (selected from a rotation photograph) having 2θ values in the range 4–26°. The equipment used is described in the next section.

X-ray Structure Determination. Single crystals of $[Et_4N][Ni(Etx)_3]$ were grown by slow diffusion of an acetone solution of the compound into hexane. A green transparent crystal was mounted. Data collection was performed on a Nicolet R3m/V automated diffractometer using graphite-monochromated Mo Kα radiation (λ = 0.71073 Å). Significant crystal data and data collection parameters are listed in Table VI. The unit cell parameters were determined by a least-squares fit of 20 reflections (selected from a rotation photograph) having 2θ values in the range 7–20°. Lattice dimensions and the Laue group were checked by axial photography. Systematic absences led to the identification of the space group as $P2_1/n$. The structure was successfully solved in this space group.

During data collection, the parameters kept fixed were as follows: ω range of 1.80°, variable scan speed between 3.0 and 30.0° min^{-1}, and ratio of background to scan time of 0.5. Two check reflections were measured after every 98 reflections during data collection to monitor the crystal stability. No significant intensity reduction was observed in the 171 h of exposure to X-rays. All data were corrected for decay (decay correction range on I was 0.9619–1.0059) and Lorentz–polarization effects. An empirical absorption correction was done on the basis of axiumuthal scans[33] of eight reflections with χ near 287° and 2θ in the range 12.5–34°.

All calculations for data reduction and structure solution and refinement were done on a MicroVAX II computer with the programs of SHELXTL-PLUS.[34] The structure was solved by direct methods. The model was then refined by full-matrix least-squares procedures. All non-hydrogen atoms were made anisotropic. Hydrogen atoms were then affixed at their idealized positions and were refined isotropically with fixed thermal parameters. The final refinement involved a scale factor, 56 anisotropic non-hydrogen atoms, and 70 isotropic hydrogen atoms. The final convergent refinement gave residuals as summarized in Table VI. The highest difference fourier peak was 0.22 e/Å^3. Atomic coordinates and isotropic equivalent thermal parameters are collected in Table VII.

Acknowledgment. We are very thankful to the Department of Science and Technology, New Delhi, for establishing a National Single Crystal Diffractometer Facility at the Department of Inorganic Chemistry, Indian Association for the Cultivation of Science. Financial support received from the Council of Scientific and Industrial Research is also acknowledged.

Supplementary Material Available: Listings of anisotropic thermal parameters (Table VIII), complete bond distances (Table IX) and angles (Table X), hydrogen atom positional parameters (Table XI), and a structure determination summary (Table XII) (11 pages); a listing of observed and calculated structure factors (34 pages). Ordering information is given on any current masthead page.

(32) Glasstone, S. *Text Book of Physical Chemistry*, 2nd ed.; Macmillan and Co. Ltd.: London, 1948.

(33) North, A. C. T.; Philips, D. C.; Mathews, F. S. *Acta Crystallogr.* **1968**, *A24*, 351–359.

(34) Sheldrick, G. M. *SHELXTL-Plus 88, Structure Determination Software Programs*; Nicolet Instrument Corp.: 5225-2 Verona Rd., Madison, WI 53711, 1988.